International Journal of Control, Automation and Systems 19(X) (2021) 1-14
http://dx.doi.org/10.1007/s12555-020-0110-9
ISSN:1598-6446 eISSN:2005-4092
http://www.springer.com/12555

Immersion and Invariance-based Sliding Mode Attitude Control of Tilt Tri-rotor UAV in Helicopter Mode

Li Yu, Guang He*, Shulong Zhao, Xiangke Wang, and Lincheng Shen

Abstract: In this paper, we propose an immersion and invariance-based sliding mode controller for a tilt tri-rotor unmanned aerial vehicle subjects to parameter perturbation, unmodeled dynamics, and external disturbances. The control scheme is divided into three parts, including the disturbance observer, the attitude controller, and the control allocation. Firstly, to alleviate the chattering and improve the robustness for attitude control, the observer using immersion and invariance theory is developed to estimate the disturbance. Note that the observer can relax the requirement of disturbance upper bound and guarantee the convergence of the estimation error. Secondly, to improve the dynamic response capability, a sliding mode attitude controller with an adaptive switch function is designed based on the disturbance observer. Thirdly, a hierarchical control allocation algorithm is proposed. The performance improvement is illustrated by comparing with other sliding mode controllers. Simulations and flight experiments are conducted to verify the effectiveness and applicability of the proposed control scheme.

Keywords: Control allocation, disturbance observer, sliding mode control, tilt tri-rotor UAV.

1. INTRODUCTION

Tilt-rotor unmanned aerial vehicle (UAV) is a novel aircraft with three flight modes, including the helicopter mode, the transition mode, and the fixed-wing mode. In the helicopter mode, it enjoys the vertical take-off and landing (VTOL) capability, so that it is not necessary for a runway, and it can be applied to many special situations such as aircraft carrier or surface warship. In the fixed-wing mode, long-distance transportation can be achieved due to its long endurance and high cruise speed. The tilt-rotor UAV that combines the advantages of the helicopter and the fixed-wing has received considerable attention in recent decades [1].

Most of the early studies are focused on dual tilt-rotor aircrafts such as XV-15 and V-22 [2]. Based on related technologies and similar configuration, the Eagle Eye and SmartUAV are developed [3–5]. However, the dual tilt-rotor UAVs have not come into extensive use due to the complicated structure and aerodynamic interference between the rotors and wings. To overcome the difficulties, more rotors are applied for relaxing the requirement of the swashplate which is an indispensable part of helicopters. The tilt tri-rotor UAV, quad tilt-rotor UAV, and tilt-wing UAV are designed for simplifying the aircraft structure and reducing the aerodynamic interference simultaneously. The quad tilt-rotor UAV has two pairs of tiltable rotors that are mounted on both sides of the fuselage [6–8], such that the aerodynamic interference can be reduced. For the tilt-wing UAV [9, 10], the rotors are assembled at the center of wings, and the rotors can tilt together with the wings to reduce the impact caused by downwash. Compared with tilt-rotor UAVs mentioned above, the tilt tri-rotor UAV has a simpler configuration, fewer actuators, and low cost. The Panther is the first tilt tri-rotor UAV, which has been delivered to the army as equipment [11]. The VTOL aircraft FireFLY6 with three pairs of rotors is a product that can be applied to the aerial photograph. Panther and FireFLY6 are two typical tilt tri-rotor UAVs that have been applied in practice. However, attitude and altitude are adjusted considerably in the transition mode, such that the stability of flight control is decreased. Taking the unstable structure and disturbances into account, the advanced control scheme should be developed for the tilt tri-rotor UAV to achieve stable flight control.

In general, the control scheme of the tilt-rotor UAV is composed of a controller and an allocator. Firstly, the high-level controller is developed to provide the virtual commands for the allocator. Secondly, the control allo-

Manuscript received February 10, 2020; revised May 19, 2020; accepted June 1, 2020. Recommended by Associate Editor Seungkeun Kim under the direction of Editor Chan Gook Park. This work is supported in part by the Natural Science Foundation of Hunan Province under grant 2019JJ50717, and the National Natural Science Foundation of China under grant 61973309.

Li Yu, Guang He, Shulong Zhao, Xiangke Wang, and Lincheng Shen are with the College of Intelligence Science and Technology, National University of Defense Technology, Changsha 410073, China (e-mails: {yulisdu, heguang410}@163.com, {jaymaths, xkwang, lcshen}@nudt.edu.cn).
* Corresponding author.

cation algorithm should be designed to map the virtual commands into the individual actuator input such that the desired moments can be generated [12]. Many efforts have been devoted to designing the flight controller for the tilt-rotor UAV with different configurations. In [8], an observer-based adaptive controller is developed for a rudderless quad tilt-rotor UAV to track the reference roll and yaw angle. Besides, the radial basis function neural network is applied to cope with the nonlinearities in the controller. In [9], by applying a controller order-reduction technique with the fractional balanced reduction to a conventional LQ optimal servomechanism, the attitude tracking controller is developed for a small prototype quad tiltwing UAV. In [13], the neural network controller for the SmartUAV is designed, and the pseudo-control hedging is introduced to improve the control performance. In [14,15], an explicit model predictive control approach relies on the constrained multiparametric optimization is proposed for a designed tilt tri-rotor UAV. In [16], the conventional PID controller and linear model predictive controller are combined for the position and attitude control of a tilt tri-rotor UAV. The control scheme can achieve effective trajectory tracking under the constraints of the states and control inputs. The robustness of the controller concerning the parameter perturbation and external disturbance is not considered in the works mentioned above. It is well known that the sliding mode control (SMC) is an effective method in dealing with the uncertainties and has been widely used for flight control [17–19]. However, the disturbance is usually assumed as a variable with known upper bound, which is not satisfied in the real flight. A large switch gain is required to ensure the robustness, and the most widely-used boundary layer technique is introduced to solve the chattering problem. The stability is obtained at the cost of sacrificing the nominal control performance [20, 21]. To alleviate the chattering and improve robustness without sacrificing control performance, the disturbance observer based on immersion and invariance (I&I) theory [22, 23] is employed to the SMC in this paper. Compared with the existing nonlinear disturbance observer (NDO) [24], and radical basic function neural network (RBFNN) [25], the observer based on I&I not only has a more concise form and fewer parameters but also has much more design freedom. It allows for prescribed uniformly stable dynamics to be assigned to the estimation error, thus leading to a modular control scheme that it is much easier to tune.

The control allocation problem of the tilt-rotor UAV with different actuators has been drawing massive attention. Many control allocation algorithms are proposed [26,27], including direct allocation, daisy-chaining, pseudoinverse allocation, quadratic programming, etc. For the control of the tri-tilt ducted fan aircraft with six actuators, the control allocation is converted into an optimization problem in [28]. Taking the actuator saturation into account, a mixed optimization objective function is designed to minimize the allocation error and power consumption. The effectiveness of the mixed optimization control allocation algorithm is verified through simulation. In [29], the control allocation is separated from the design of the controller to achieve stable control of the tilt-rotor UAV. By distributing residual control to the redundant actuators, a devised daisy-chaining method is proposed to cope with actuator saturation. In [30], a modular control allocation framework is developed for an incremental nonlinear dynamic inversion baseline controller, and a pseudoinverse allocation algorithm is derived to handle saturation. Flight experiment results show that the demanded inputs are appropriately allocated. Most of the control allocation algorithms are based on the optimization formulation. However, the optimization control allocation algorithm is difficult to be applied in a small aircraft with limited computing capacity. Besides, the conventional allocation algorithms can not deal with the nonlinear allocation problem in the flight control of the tilt tri-rotor UAV. To achieve a precise allocation, a modified hierarchical pseudoinverse allocation algorithm considering the dynamic characteristics of different actuators is proposed, and the analytical solution is also provided.

In this paper, an immersion and invariance-based sliding mode controller (SMCII) is proposed to improve the attitude control performance of tilt tri-rotor UAV in the presence of parameter perturbation, unmodeled dynamics, and external disturbances. First of all, the disturbance observer using I&I theory is constructed to alleviate the chattering and improve the robustness. To the best of our knowledge, the I&I theory is generally used for parameter estimation and has not been applied to estimate disturbance in practice. Secondly, an SMCII controller with an adaptive switch function is developed to ensure the stability of the attitude system. Finally, by considering the dynamic characteristics of actuators, a hierarchical allocation algorithm is proposed to map the inputs of actuators to the commands given by the controller. The main contributions of this paper are summarized as follows:

(i) The I&I-based disturbance observer is proposed for the tilt tri-rotor UAV to deal with different kinds of disturbances. The convergence of the estimation error is always guaranteed with proven stability. By introducing the I&I-based disturbance observer, the chattering can be alleviated without sacrificing the nominal control performance.

(ii) An adaptive switch function based on the disturbance observer is developed for the SMCII controller to improve the dynamic response capability. The adaptive term in the SMCII controller can adjust autonomously with respect to the disturbance error, thus the prior knowledge of the disturbance is not required.

(iii) A hierarchical control allocation algorithm considers the dynamic characteristics of actuators is developed

and applied in the real flight, in which an analytical solution can be obtained for the nonlinear control allocation problem.

The remaining sections are arranged as follows: Section 2 describes the configuration and mathematical model of the tilt tri-rotor UAV. Section 3 illustrates the design of the controller and the stability analysis in detail. The design of the control allocation algorithm is shown in Section 4. Section 5 presents the results of the simulations and flight experiments to support the theoretical developments. Concluding remarks are given in Section 6.

2. MODEL DESCRIPTION

This section describes the configuration of the tilt tri-rotor UAV and derives the corresponding dynamic model. The tilt tri-rotor UAV is an aircraft with three tiltable rotors, in which the control principle is more complicated than conventional aircraft. To further understand the aircraft, we first illustrate the principle of flight based on the 3D modeling software. And then, the force and moment generated during the flight are calculated. Finally, the mathematical model is derived according to the Newton-Euler formulation.

2.1. Configuration description

The tilt tri-rotor UAV has three flight modes that are controlled with different schemes. In the helicopter mode, position control is achieved by the adjustment of attitude. Fig. 1 shows the concept of attitude control in the helicopter mode.

There are six actuators, including three rotors and three servos can be used to control attitude. The right rotor and rear rotor rotate in counterclockwise while the left in clockwise. The two front rotors and the rear rotor can tilt from $\pi/6$ to $-\pi/2$ with respect to the vertical axis. The interference between rotors and wings can be ignored due to the distance from the wing to the rotor is long enough. Note that this study focuses only on the attitude control of the aircraft in helicopter mode. Roll motion is achieved by adjusting the thrust of the left and right rotors. The rear rotor is used to compensate for the moment generated by two front rotors to stabilize the pitch. The yaw moment is created by the difference of tilting angles between front rotors. Besides, the altitude is controlled by adjusting the thrust of all rotors.

2.2. Nonlinear equations of motion

The dynamic model of the tilt tri-rotor UAV is complex due to its time-varying structure. The design of the controller and allocator is based on the system model so that the dynamic and kinematic equations should be derived first. Fig. 2 shows the coordinate systems of the aircraft. The term Σ_e represents the world coordinate system, Σ_b denotes the body coordinate system, and Σ_{ri} represents the rotor coordinate system. It is noted that the right rotor, the left rotor, and the rear rotor are labeled by 1, 2, 3, respectively. The tilting angles $[\alpha_1, \alpha_2, \alpha_3]^T$ are defined as negative when the two front rotors tilt forward, or the rear rotor tilts backward. The transformation from the rotor frame to the body frame is denoted using the matrix R_{ri}^b as follows:

$$R_{ri}^b = \begin{bmatrix} \cos\alpha_i & 0 & \sin\alpha_i \\ 0 & 1 & 0 \\ -\sin\alpha_i & 0 & \cos\alpha_i \end{bmatrix}, \ i = 1,2,3. \tag{1}$$

In the helicopter mode, the aerodynamic force generated by wings is small enough compared to the thrust and gravity, so that it can be ignored. The force F^b contains the rotor thrust F_{ri}^b and gravity F_g^b.

$$F^b = F_g^b + F_{r1}^b + F_{r2}^b + F_{r3}^b, \tag{2}$$

$$F_g^b = mg \cdot R_{EBT} \cdot \rho, \tag{3}$$

$$F_{ri}^b = -k_f \omega_i^2 \cdot R_{ri}^b \cdot \rho, \tag{4}$$

where R_{EBT} denotes the transformation matrix from the world frame to the body frame, the mass of the platform is expressed as m, and g denotes the gravitational acceleration. Note that k_f represents the thrust coefficient of rotor, ω_i represents the rotational angular velocity of rotor i,

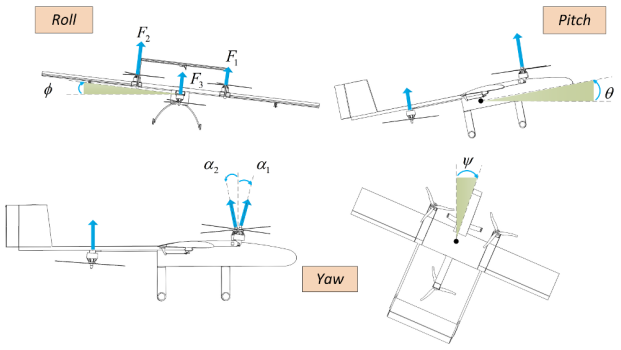

Fig. 1. Attitude control principle.

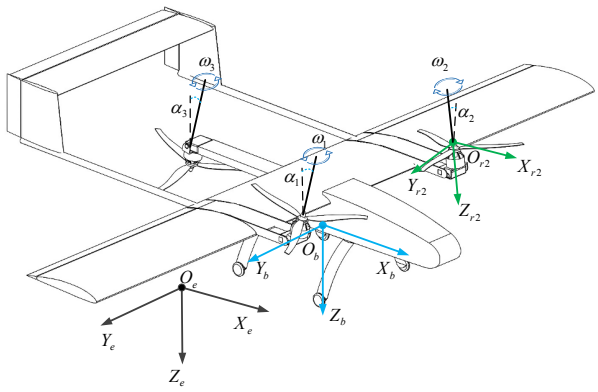

Fig. 2. Tilt tri-rotor UAV coordinate system.

and ρ is the constant vector $[0,0,1]^T$. The term τ^b consists of the moment created by the thrust of rotor τ_F^b, reaction torque of rotor τ_d^b, and the gyroscopic moment τ_G^b.

$$\tau^b = \tau_F^b + \tau_d^b + \tau_G^b, \tag{5}$$

where

$$\tau_F^b = \sum_{i=1}^{3} L_i^b \times F_{ri}^b, \tag{6}$$

$$\tau_d^b = k_d\omega_1^2 \cdot R_{r1}^b \cdot \rho - k_d\omega_2^2 \cdot R_{r2}^b \cdot \rho + k_d\omega_3^2 \cdot R_{r3}^b \cdot \rho, \tag{7}$$

$$\tau_G^b = \sum_{i=1}^{3} J_r\Omega_i \times (\Omega_b + \Omega_{si}). \tag{8}$$

In these equations, $L_i^b = [r_{ix}, r_{iy}, r_{iz}]^T$ denotes the position of rotor i in the body frame, k_d represents the torque coefficient of rotor, J_r is the moment of inertia of the rotor, Ω_i represents the rotational angular velocity of rotor i in the body frame and can be expressed as $\Omega_i = (-1)^i\omega_i[\sin\alpha_i, 0, \cos\alpha_i]^T$, $\Omega_b = [p,q,r]^T$ represents the angular velocity of the aircraft, Ω_{si} is the tilting angular velocity of rotor i. According to the Newton-Euler formulation, the dynamic model of the tilt tri-rotor UAV is derived as

$$\begin{cases} \dot{\Theta} = R_{BER} \cdot \Omega_b, \\ I_b\dot{\Omega}_b = \Gamma - \Omega_b \times (I_b \cdot \Omega_b) + d_\Gamma, \end{cases} \tag{9}$$

where $\Gamma = [R,P,Y]^T$ is the virtual control torque, d_Γ represents the external disturbance, $\Theta = [\phi,\theta,\psi]^T$ is the Euler angle, $I_b \in R^{3\times3}$ is the inertial matrix with respect to the body frame. The rotation matrix from the body frame to the world frame is given as

$$R_{BER} = \begin{bmatrix} 1 & \sin\phi\tan\theta & \cos\phi\tan\theta \\ 0 & \cos\phi & -\sin\phi \\ 0 & \dfrac{\sin\phi}{\cos\theta} & \dfrac{\cos\phi}{\cos\theta} \end{bmatrix}. \tag{10}$$

3. I&I-BASED SLIDING MODE CONTROLLER

In this study, the control scheme is developed based on two steps. The first step is to develop a controller specifying virtual control commands. Then, the second step is to design a control allocation algorithm that maps the virtual control commands on individual actuators. In this section, the design of the attitude controller is divided into two parts. First, an observer based on I&I is designed to estimate the disturbance. Second, the sliding mode control law with an adaptive switch function is developed. The proposed SMCII controller has two powerful properties over the conventional SMC controller with the boundary layer technique. On the one hand, the prior knowledge of the upper bound of disturbance is not required, which can improve the adaptive ability of the control system. On the other hand, the chattering can be alleviated without sacrificing nominal control performance. Note that we focus only on the development of the attitude controller. The desired angle $[\phi_r, \theta_r, \psi_r]^T$ and command T are given by the position controller. A block diagram of the developed control scheme is shown in Fig. 3.

3.1. Disturbance observer

In this section, a nonlinear observer based on I&I is proposed to estimate the disturbance. Taking the modeling error and the external disturbance into account, the attitude system (9) can be rewritten as follows:

$$\begin{aligned} (J_0(\Theta) + J_\triangle(\Theta))\ddot{\Theta} = &-(C_0(\Theta,\dot{\Theta}) + C_\triangle(\Theta,\dot{\Theta}))\dot{\Theta} \\ &+ \Gamma + d_\Gamma, \end{aligned} \tag{11}$$

where $J_0(\Theta) \in R^{3\times3}$ denotes the moment of inertia in the world frame, $\Theta = [\phi,\theta,\psi]^T$ is the actual Euler angle, $C_0(\Theta,\dot{\Theta}) \in R^{3\times3}$ denotes the Coriolis matrix, $\Gamma = [R,P,Y]^T$ represents virtual control command which is the output of the attitude controller, and d_Γ is the external disturbance. Note that $J_\triangle(\Theta)$ and $C_\triangle(\Theta,\dot{\Theta})$ are produced due to modeling error. Equation (11) can be simplified as

$$J_0(\Theta)\ddot{\Theta} = -C_0(\Theta,\dot{\Theta})\dot{\Theta} + \Gamma + d, \tag{12}$$

where $d = d_\Gamma - J_\triangle(\Theta)\ddot{\Theta} - C_\triangle(\Theta,\dot{\Theta})\dot{\Theta}$. The term $J_0(\Theta)$ can be derived from the inertial matrix I_b through coordinate transformation.

$$J_0(\Theta) = \begin{bmatrix} I_x & 0 \\ 0 & I_y c^2\phi + I_z s^2\phi \\ -I_x s\theta & (I_y - I_z)c\phi s\phi c\theta \end{bmatrix}$$

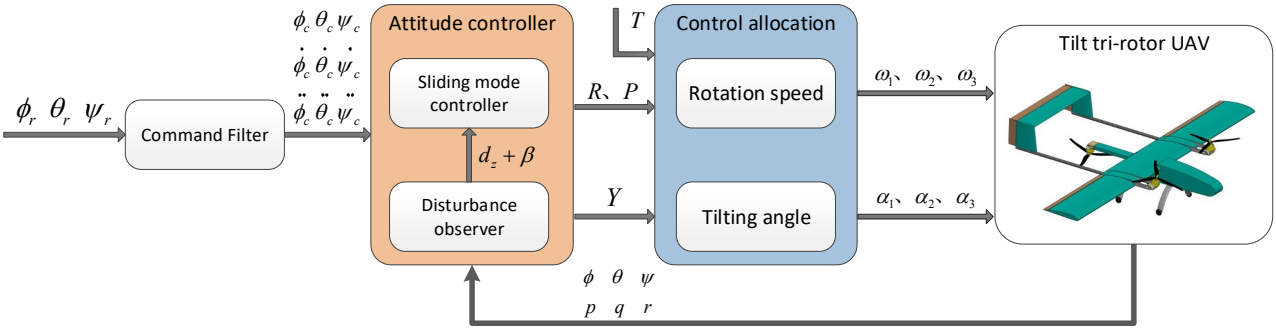

Fig. 3. Structure of the overall control scheme.

$$\begin{bmatrix} -I_x s\theta \\ (I_y - I_z)c\phi s\phi c\theta \\ I_x s^2\theta + (I_y s^2\phi + I_z c^2\phi)c^2\theta \end{bmatrix} \tag{13}$$

where $c\cdot$ and $s\cdot$ symbolize cosine and sine function, respectively. So that the determinant of $J_0(\Theta)$ can be obtained

$$|J_0(\Theta)| = I_x I_y I_z \cos^2\theta. \tag{14}$$

Without loss of generality, the pitch angle satisfies $\theta \in (-\pi/2, \pi/2)$, therefore, $J_0(\Theta)$ is a positive definite symmetric matrix. According to the nature of the positive definite symmetric matrix, $J_0(\Theta)$ is invertible, and $J_0(\Theta)^{-1}$ is a positive definite symmetric matrix too.

Define the angle error $X_1 = \Theta - \Theta_c$ and the angular velocity error $X_2 = \dot{\Theta} - \dot{\Theta}_c$. It follows from (12) that the attitude error system satisfies

$$\begin{cases} \dot{X}_1 = X_2, \\ \dot{X}_2 = J_0(\Theta)^{-1}(\Gamma + d - C_0(\Theta,\dot{\Theta})(X_2 + \dot{\Theta}_c) \\ \qquad - J_0(\Theta)\ddot{\Theta}_c). \end{cases} \tag{15}$$

Assumption 1: The composite disturbance is composed of parameter uncertainties and external disturbances, which derivative is bounded as $\|\dot{d}\| \leq \xi$, where ξ is a positive constant.

According to [31], the disturbance estimation error $z = [z_1, z_2, z_3]^T$ can be defined as

$$z = d_z + \beta(X_1, X_2) - d, \tag{16}$$

where $d_z \in R^3$ is the dynamic part, and $\beta(X_1, X_2) \in R^3$ is an auxiliary function which will be designed later. The derivative of z along (15) satisfies

$$\begin{aligned} \dot{z} =& \dot{d}_z + \frac{\partial \beta}{\partial X_1} X_2 + \frac{\partial \beta}{\partial X_2} J_0(\Theta)^{-1}(\Gamma + d_z + \beta(X_1, X_2) \\ & - z - C_0(\Theta,\dot{\Theta})(X_2 + \dot{\Theta}_c) - J_0(\Theta)\ddot{\Theta}_c) - \dot{d}. \end{aligned} \tag{17}$$

Theorem 1: To achieve accurate estimation of the disturbance, the adaptive update law $\dot{d}_z$ and auxiliary function $\beta(X_1, X_2)$ can be designed as follows:

$$\begin{aligned} \dot{d}_z =& -\frac{\partial \beta}{\partial X_1} X_2 - \frac{\partial \beta}{\partial X_2} J_0(\Theta)^{-1}(\Gamma + d_z + \beta(X_1, X_2) \\ & - C_0(\Theta,\dot{\Theta})(X_2 + \dot{\Theta}_c) - J_0(\Theta)\ddot{\Theta}_c), \end{aligned} \tag{18}$$

$$\beta(X_1, X_2) = k_1 E + k_2 X_2, \tag{19}$$

where $E = X_1 \circ X_1 \circ X_2$ (Hadamard product), k_1 and k_2 are positive constants that related to the convergence rate of the disturbance estimation.

Proof: Assign a Lyapunov function candidate

$$V_z = \frac{1}{2} z^T z. \tag{20}$$

After taking the time derivative of (20) and substituting (17)-(19) into the resulting equation, the derivative of the Lyapunov function can be written as

$$\begin{aligned} \dot{V}_z &= z^T \dot{z} \\ &= -z^T \Lambda J_0(\Theta)^{-1} z - z^T \dot{d} \\ &\leq -\|z\|(\lambda_{min}\|z\| - \xi), \end{aligned} \tag{21}$$

where $\Lambda = \dfrac{\partial \beta}{\partial X_2}$ is a positive definite diagonal matrix, and its elements can be represented as $\Lambda(i,i) = k_1 X_1^2(i) + k_2, i = 1,2,3$. Due to $J_0(\Theta)^{-1}$ is a positive definite symmetric matrix, so it is obvious that $\Lambda J_0(\Theta)^{-1} > 0$. λ_{min} is the smallest eigen value of $\Lambda J_0(\Theta)^{-1}$. According to the inequality (21), we can conclude that the estimation error is bounded by $\|z\| \leq \xi/\lambda_{min}$. Note that the estimation error can converge to zero if the disturbance is constant. □

Remark 1: The auxiliary function $\beta(X_1, X_2)$ can be designed in different forms to ensure the convergence of the estimation error. In this paper, the proposed auxiliary term $\beta(X_1, X_2)$ is a nonlinear function of X_1 and X_2, and the elements of the matrix Λ are bigger when the states far away from the equilibrium point. The designed auxiliary function $\beta(X_1, X_2)$ contributes to improving the convergence rate of the disturbance estimation.

3.2. Design of sliding mode controller based on disturbance observer

In the following, the objective is to develop the sliding mode controller based on the disturbance observer, such that the chattering is alleviated and robustness can be improved without sacrificing nominal control performance. To deal with the chattering problem, the disturbance observer is used to compensate for external disturbances and parameter uncertainties. In order to improve the dynamic response capability, an adaptive switch function is proposed according to the auxiliary function $\beta(X_1, X_2)$. Based on the attitude error system (15), the sliding mode surface is defined as

$$s = X_2 + kX_1, \tag{22}$$

where k is a positive constant. The observer provides the disturbance estimation $d_z + \beta(X_1, X_2)$, and the auxiliary function $\beta(X_1, X_2)$ is a nonlinear function that related to the convergence rate of the disturbance estimation.

Assumption 2: The disturbance estimation error is bounded and defined by $e_d^* = \sup_{t>0} |d_z + \beta(X_1, X_2) - d|$.

Taking (19) into consideration, it shows that if the system states converge to the equilibrium point asymptotically, the value of the auxiliary function $\beta(X_1, X_2)$ will approach zero. To improve the dynamic response capability and attenuate chattering simultaneously, an adaptive

switch function is designed as follows:

$$\varepsilon(t) = \delta diag(|\beta_i(X_1, X_2)|) + \varepsilon_0 I, \tag{23}$$

where δ and ε_0 are positive constants, $\varepsilon_0 \geq e_d^*$, and I is an identity matrix.

Theorem 2: To alleviate the chattering and improve robustness without sacrificing the nominal performance, the SMC method and disturbance observer are combined to develop the control law which is given by

$$\begin{aligned}\Gamma =& C_0(\Theta, \dot{\Theta})(X_2 + \dot{\Theta}_c) + J_0(\Theta)(\ddot{\Theta}_c - kX_2) \\ & - cs - \varepsilon(t) sgn(s) - (d_z + \beta(X_1, X_2)),\end{aligned} \tag{24}$$

where c is a positive definite diagonal matrix, and the adaptive switch function is introduced to the control law.

Proof: Taking the derivative of the sliding mode surface s along the attitude system (15) yields

$$\begin{aligned}\dot{s} =& \dot{X}_2 + k\dot{X}_1 \\ =& kX_2 + J_0(\Theta)^{-1}\big(\Gamma + d - C_0(\Theta, \dot{\Theta})(X_2 + \dot{\Theta}_c) \\ & - J_0(\Theta)\ddot{\Theta}_c\big).\end{aligned} \tag{25}$$

Substituting the control law (24) into (25) yields

$$\begin{aligned}\dot{s} =& J_0(\Theta)^{-1}\big[-cs - \varepsilon(t) sgn(s) + d \\ & - (d_z + \beta(X_1, X_2))\big].\end{aligned} \tag{26}$$

Consider a candidate Lyapunov function as

$$V_s = \frac{1}{2} s^T s. \tag{27}$$

The derivative of the Lyapunov function along (26) satisfies

$$\begin{aligned}\dot{V}_s =& s^T J_0(\Theta)^{-1}\big[-cs - \varepsilon(t) sgn(s) + d \\ & - (d_z + \beta(X_1, X_2))\big].\end{aligned} \tag{28}$$

It is worth noting that $\varepsilon_0 \geq e_d^*$, $J_0(\Theta)^{-1}$ is a positive definite symmetric matrix. According to the definition of the adaptive switch function (23), it is obvious that

$$\begin{aligned}\dot{V}_s \leq& -s^T J_0(\Theta)^{-1} cs \\ & - s^T J_0(\Theta)^{-1} \delta diag(|\beta_1|, |\beta_2|, |\beta_3|) sgn(s) \\ \leq& 0.\end{aligned} \tag{29}$$

It can be concluded that the sliding mode surface $s = X_2 + kX_1$ converges to the equilibrium point asymptotically under the proposed control law (24). Since the reachability condition of the sliding mode surface is satisfied, $X_2 + kX_1 = 0$ implies that X_1 converges to zero asymptotically with the rate of k. □

Remark 2: The adaptive switch function (23) is introduced to the control law, and the value of this adaptive term varies with system states. If the states far away from the equilibrium point, the switch gain increases to improve dynamic response. On the other hand, the switch gain approaches to ε_0 to avoid chattering when the states around the equilibrium point.

Remark 3: In general, the switch gain of the SMC must be designed bigger than the amplitude of disturbance to guarantee stability. The disturbance is estimated in this paper, and the estimation error is smaller than the bound of d. So that the constant ε_0 can be designed much smaller than the conventional SMC, and the chattering can be alleviated effectively. The control law (24) reduces to a baseline SMC in the absence of disturbance, which means that the control scheme can maintain nominal performance.

4. CONTROL ALLOCATION

In this section, the design of the control allocation algorithm which provides the mapping from the virtual control commands to the manipulated inputs of the aircraft is presented. Similar to a conventional aircraft, the tilt tri-rotor UAV has four virtual control commands R, P, Y and T, where R is directly linked to the control of roll motion, P is used for pitch control, Y is related to yaw control, and the altitude is controlled by T. The virtual control vector $[R, P, Y]^T$ is given by the attitude controller, while the virtual thrust T comes from the position controller. In the helicopter mode, the tilt tri-rotor UAV has six actuators that consist of three rotors and three servos, and there are four virtual control commands need to be allocated. Due to the response speed of the rotor and servo are different, the calculation of actual inputs can be divided into two parts.

For the first part, the rotation speed of three rotors are acquired according to R, P and T. It is noted that the tilting angles are estimated before calculating the rotation speed $[\omega_1^2, \omega_2^2, \omega_3^2]^T$. By

$$\begin{bmatrix} R \\ P \\ T \end{bmatrix} = \Delta \begin{bmatrix} \omega_1^2 \\ \omega_2^2 \\ \omega_3^2 \end{bmatrix}, \tag{30}$$

where

$$\Delta = \begin{bmatrix} -k_f r_{1y} c\alpha_1 + k_d s\alpha_1 & -k_f r_{2y} c\alpha_2 - k_d s\alpha_2 & k_d s\alpha_3 \\ k_f r_{1x} c\alpha_1 & k_f r_{2x} c\alpha_2 & k_f r_{3x} c\alpha_3 \\ k_f c\alpha_1 & k_f c\alpha_2 & k_f c\alpha_3 \end{bmatrix}, \tag{31}$$

where $c\cdot$ and $s\cdot$ symbolize cosine and sine function respectively. Since the matrix Δ is a square matrix, the key point

to obtain rotation speed $[\omega_1^2, \omega_2^2, \omega_3^2]^T$ is to verify the reversibility of the matrix Δ. In the helicopter mode, the angle $\alpha_3 = 0$, and it is reasonable to assume that $\alpha_1 + \alpha_2 = 0$. In this manner, the determinant of the matrix Δ can be written as follows:

$$|\Delta| = -2k_f^3 r_{1y}(r_{1x} - r_{3x})(\cos\alpha_1)^2. \tag{32}$$

The tilting angles are limited to $(-\pi/6, \pi/6)$ in helicopter mode, namely $cos\alpha_1 \geq \sqrt{3}/2$. Besides, considering the condition $r_{1x} \neq r_{3x}$, we can conclude that

$$|\Delta| \neq 0. \tag{33}$$

The reversibility of the matrix Δ is proved, so that the rotation speed can be obtained by

$$\begin{bmatrix} \omega_1^2 \\ \omega_2^2 \\ \omega_3^2 \end{bmatrix} = \Delta^{-1} \begin{bmatrix} R \\ P \\ T \end{bmatrix}. \tag{34}$$

For the second part, two tilting angles need to be determined based on the yaw command Y and rotation speed $[\omega_1^2, \omega_2^2, \omega_3^2]$. It is worth noting that the term $\alpha_1 + \alpha_2$ may not rigorously remain zero due to the existence of installation error and measurement error. However, these errors are small enough and can be handled by the proposed controller. According to the assumption $\alpha_1 + \alpha_2 = 0$, two methods can be applied to acquire tilting angles. The moment balance method is based on the assumption that tilting angles are small enough. The derivation of tilting angles depends on the value of rotation speed of three rotors. On the contrary, the proportion control method does not rely on the rotation speed, and the decoupling makes it easier to control yaw motion in real flight.

Moment balance method:

$$\begin{aligned} Y =& k_f(\omega_1^2 r_{1y}\sin\alpha_1 + \omega_2^2 r_{2y}\sin\alpha_2) \\ &+ k_d(\omega_1^2\cos\alpha_1 - \omega_2^2\cos\alpha_2 + \omega_3^2). \end{aligned} \tag{35}$$

In general, the value of the rotation speed $[\omega_1^2, \omega_2^2, \omega_3^2]^T$ is difficult to be obtained. However, the control input of the rotor is a known quantity for the control system. The rotation speed corresponding to the maximum input is denoted by a constant ω_{max}, so that the term $\eta_i = \omega_i/\omega_{max}(i = 1,2,3)$ can be derived based on the control input of different rotors. In the helicopter mode, a small differential angle between two front rotors can generate enough moment to adjust yaw motion. It is reasonable to assume that tilting angles are small, so that we have

$$\begin{cases} \sin(\alpha_i) \approx \alpha_i, \\ \cos(\alpha_i) \approx 1. \end{cases} \tag{36}$$

Combined with the assumption $\alpha_1 + \alpha_2 = 0$, the tilting angle α_1 can be obtained according to (35) as follows:

$$\alpha_1 = \frac{\dfrac{Y}{\omega_{max}^2} - k_d(\eta_1^2 - \eta_2^2 + \eta_3^2)}{k_f(r_{1y}\eta_1^2 - r_{2y}\eta_2^2)}. \tag{37}$$

Proportion control method:

Considering the fact that the yaw motion can be adjusted effectively by tilting the two front rotors in opposite directions. From this point of view, the tilting angle is given as follows:

$$\alpha_1 = \delta \cdot Y, \tag{38}$$

where δ is a small constant that depends on the maximum tilting angle and the corresponding yaw moment.

The two methods derived above can be used for the control of the aircraft. However, the proportion control method only needs the value of yaw command Y, so that it is easier to be applied compared to the moment balance method. Note that the command Y is not equal to zero when hovering due to the torque created by the rear rotor, and the torque can be compensated by the observer. Taking the reliability and simplicity into account, the proportion control method is applied in the simulation and flight experiment.

5. SIMULATION AND FLIGHT EXPERIMENT

The results of the simulations and flight experiments are presented in this section. A disturbance observer based on I&I is used to compensate for the parameter perturbation, unmodeled dynamics, and external disturbances. The adaptive switch function is introduced for the controller to improve the dynamic response capability. The hierarchical allocation algorithm is applied to simplify the design of the control system. To validate the performance of the proposed control scheme, numerical simulation and experiments are carried out.

A prototype is built to verify the proposed control scheme, and the parameters of the aircraft are obtained by combining various methods. The moments of inertia about the X and Y axis are acquired by the compound-pendulum method. Moreover, the moment of inertia about the Z axis is obtained by the bifilar torsion pendulum method. The propulsion system consists of a motor and a propeller is tested by an intelligent ergometer that can record the value of force, moment, and rotation speed. Data are acquired after the test of the propulsion system, and then the thrust coefficient k_f and torque coefficient k_d can be obtained by using the least square method [32]. The value of the tilting angle is necessary for precision control allocation. However, for the platform, it is difficult to install a sensor due to its unique structure. Considering the fact that the tilting angle changes linearly with the actual input so that we can estimate the tilting angle according to the actual input given by allocator. The rear rotor is fixed vertically in the helicopter mode, and the parameters of the tilt tri-rotor UAV are shown in Table 1. Note that the position of rotor 2 can be derived from rotor 1 due to the symmetrical structure of the aircraft.

Table 1. Parameters of the tilt tri-rotor UAV.

Symbol	Magnitude	Units
m	5.900	kg
r_{1x}	0.195	m
r_{1y}	0.315	m
r_{1z}	0.000	m
r_{3x}	−0.490	m
r_{3y}	0.000	m
r_{3z}	0.000	m
I_x	0.311	kg·m^2
I_y	0.485	kg·m^2
I_z	0.660	kg·m^2
k_f	4.531×10^{-5}	N / (rad/s)^2
k_d	9.409×10^{-7}	(N·m) / (rad/s)^2

5.1. Simulation verification

In this section, the proposed SMCII controller is applied to stabilize the tilt tri-rotor UAV that subjects to parameter perturbation, unmodeled dynamics, and external disturbances. The mathematical model is obtained based on the prototype which is designed in the laboratory. Without loss of generality, different types of disturbances are considered and introduced to the system simultaneously. Firstly, the modeling error is inevitable, which means that the parameter perturbation must be taken into account. The parameter perturbation can decrease the accuracy of the allocation so that the control performance is influenced to some extent. Secondly, the tilting rotors are driven by two servos respectively, the wheel clearance and the estimation error of the tilting angle are difficult to be eliminated in the real flight. Thirdly, the external disturbance should be considered when discussing the performance of the control scheme. Finally, the actuators in real flight have different settling times, so the time delay problem should be considered.

Several significant parameters are changed as shown in Table 2, which is used to describe the parameter perturbation. To study the influence caused by the wheel clearance and the estimation error of the tilting angle, a random function (−0.05 rad-0.05 rad) is used to represent the uncertainties of the tilting angle. The external disturbance given in (39) is applied to the attitude system. Taking the time delay problem exists in the real flight into account, the time delay of 0.03 seconds and 0.018 seconds for the rotor and servo are introduced to the simulation. Different types of disturbances listed above are applied to the control system simultaneously, which can mostly simulate the real condition and verify the control performance.

Table 2. Parameter perturbation.

Symbol	Variation	Symbol	Variation
r_{1x}	+20%	b	+20%
r_{1y}	−20%	d	−20%
r_{2x}	+20%	I_x	−20%
r_{2y}	−20%	I_y	−20%
r_{3x}	+20%	I_z	−20%

$$d_\Gamma = \begin{bmatrix} 1.5\sin(2t) - 1.5\cos(2t) \\ 1.5\sin(2t) + 1.5\cos(2t) \\ 1.5\sin(2t) \end{bmatrix} \text{ N·m} \tag{39}$$

To show the performance improvement obtained with the proposed controller, simulations are conducted by comparing the proposed SMCII with the sliding mode controller based on nonlinear disturbance observer (SMC-NDO) [24], the sliding mode controller based on radical basic function neural network (SMC-RBFNN) [25], and the conventional SMC with boundary layer technique [20]. The initial attitude of the tilt tri-rotor UAV is given by $[\phi_0, \theta_0, \psi_0] = [-0.2, -0.2, -0.2]$, and the step signal is applied as the reference input. To assess the controller's performance directly, two performance indices including the Integral-Absolute-Error (IAE) $IAE_x = \int_0^T |x|dt$ and the Integral-Time-Absolute-Error (ITAE) $ITAE_x = \int_0^T |x|tdt$ are introduced. The less IAE means faster convergence rate, and the less ITAE means higher control accuracy of the steady-state. Hence, these two indices are considered here simultaneously to evaluate the control performance of different controllers.

In the presence of disturbances, the tracking results under different controllers are shown in Fig. 4. Besides, the corresponding performance indices of these controllers are provided in Fig. 5 and Fig. 6 to acquire more insights on the effectiveness of the controllers. Note that the IAE index is applied to evaluate the convergence

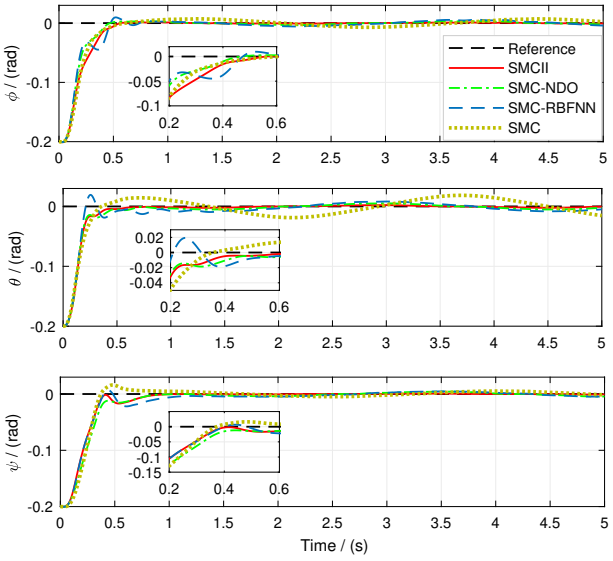

Fig. 4. Attitude tracking results in the presence of disturbances.

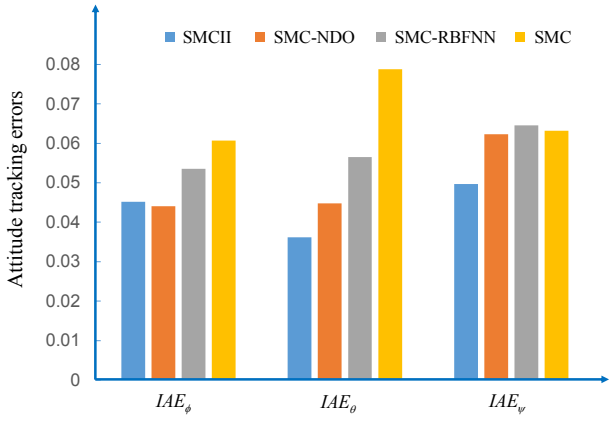

Fig. 5. Comparison of the IAE index.

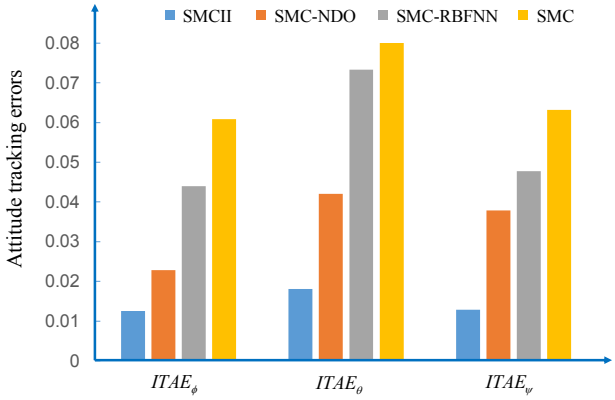

Fig. 6. Comparison of the ITAE index.

rate, and the ITAE index is used to assess the control accuracy. Taking the indices of the conventional SMC and the proposed SMCII for example. The IAE indices on three channels are $(0.06069, 0.07881, 0.06319)$ and $(0.04521, 0.03618, 0.04965)$ for the SMC and SMCII, respectively. It can be observed that the performance is improved by the SMCII for all states ($\phi \downarrow 25.51\%, \theta \downarrow 54.09\%, \psi \downarrow 21.43\%$). For the SMC and SMCII, the ITAE indices are $(0.06088, 0.1324, 0.04354)$ and $(0.01256, 0.01811, 0.01282)$. The tracking accuracy is improved by the SMCII for all states ($\phi \downarrow 79.37\%, \theta \downarrow 86.32\%, \psi \downarrow 70.56\%$). According to the two performance indices presented in the figures, it is observed that the proposed SMCII can achieve better control performance than the SMC-NDO and SMC-RBFNN too.

The outputs of three rotors and two front servos are shown in Figs. 7 and 8, respectively. It should be mentioned that the four controllers can alleviate the chattering effectively, and the curves of actuators have a similar varying tendency under the influence of the disturbances. It can be seen that the oscillation of the tilting angles is caused by the wheel clearance and the angle estimation error. The disturbance observer contributes to enhancing the robust-

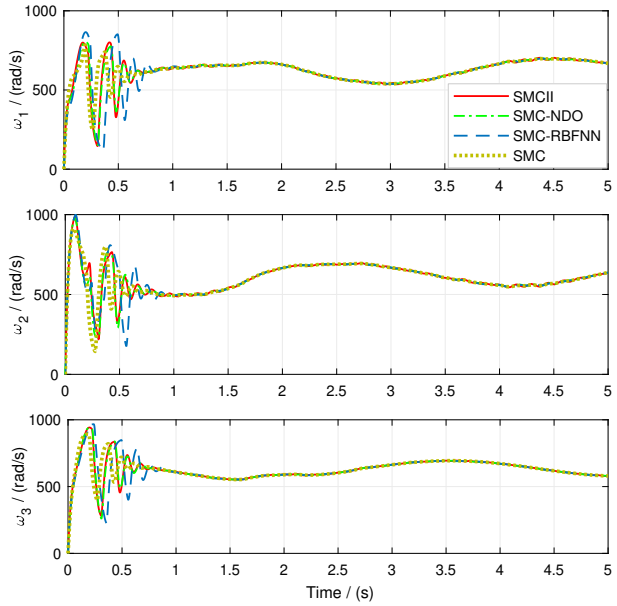

Fig. 7. Angular velocity of three rotors.

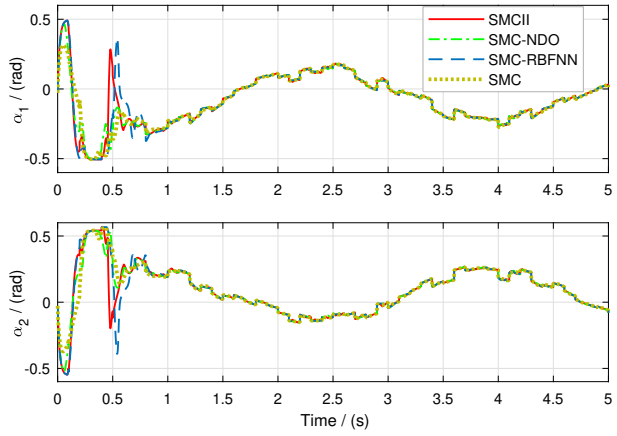

Fig. 8. Tilting angle of two front rotors.

ness and alleviating the chattering simultaneously. The estimation of disturbance using different controllers is given in Fig. 9. It should be noted that the total disturbance consists of parameter perturbation, unmodeled dynamics, and external disturbances, however, the disturbance shown in the figure denotes the external disturbance d_Γ that usually plays the main part. For the yaw-axis, due to the torque of the rear rotor is regarded as disturbance under the proportion control method, so that there always existing a small error between estimation and external disturbance. The estimation errors of the roll-axis and pitch-axis are mainly caused by the parameter perturbation. It can be seen that the proposed controllers can obtain information on the external disturbance at a faster rate and higher accuracy.

According to the simulation results, SMCII and another three controllers can achieve stable control of the attitude

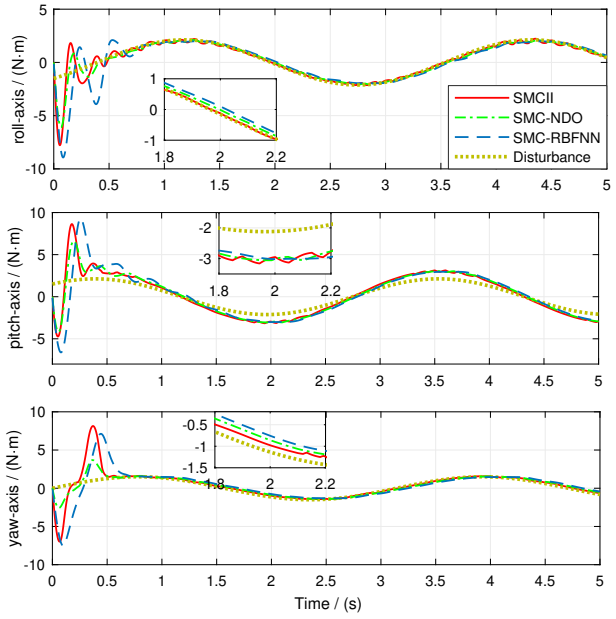

Fig. 9. Disturbance estimation.

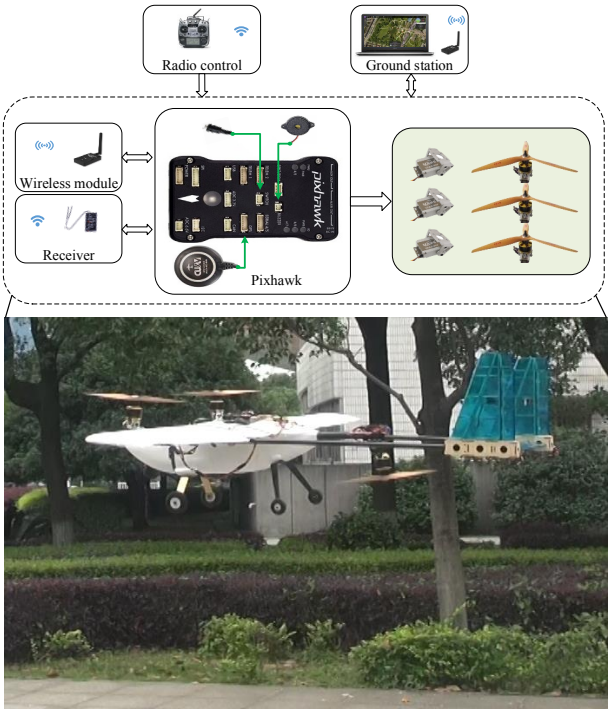

Fig. 10. Configuration of the experiment.

in the presence of disturbances. However, the robustness of the conventional SMC controller depends on the large switch gain, and the chattering is alleviated at the cost of control performance. The disturbance observer of the SMCII controller contributes to enhancing the robustness and reducing chattering. Besides, the adaptive switch function based on the observer can improve the dynamic response capability. The simulation results have demonstrated the superiority of the proposed control system. To verify the effectiveness and practicability of the proposed control scheme further, experiments are carried out on the tilt tri-rotor UAV.

5.2. Experimental results

In this subsection, the proposed control scheme SMCII and the conventional SMC are tested on a tilt tri-rotor UAV to further verify the effectiveness and superiority of the proposed control scheme. The onboard autopilot is based on the Pixhawk flight controller which contains a 168-MHz ARM processor, a 3-axis gyroscope, a 3-axis accelerometer, and a 3-axis magnetometer. The memory card in the autopilot is used to record the flight data. A ground control station is connected with the aircraft by wireless digital communication module so that the flight control parameters can be modified online. To ensure flight safety, the aircraft is controlled manually, such that the desired attitude angles can be provided by the remote device. The configuration of the experiment is depicted in Fig. 10.

Based on the tilt tri-rotor UAV, two experiments are completed, respectively. Note that the experiments are conducted in the same conditions. The aircraft is controlled manually by a remote control device, and the flight data within continuous 50 seconds are extracted for comparison and analysis. In the first experiment, the conventional SMC controller is applied to control the attitude of the tilt tri-rotor UAV. Attitude tracking results are depicted in Fig. 11(a), and the tracking errors are shown in Fig. 12(a). One can see that there are steady-state tracking errors with $0.1rad$ in the roll and pitch axis. Furthermore, the curve of the yaw tracking error has a significant fluctuation when $\psi = \pm\pi$. It should be mentioned that the fluctuation is caused by the definition of the yaw angle $(-\pi \sim +\pi)$.

As is well known, the SMC controller with appropriate control parameters is insensitive to the matched uncertainties. However, the robustness depends on the switch gain, and the increase of the switch gain tends to cause the chattering problem and make the system have a large overshoot even unstable. Besides, there are many mismatched uncertainties in the real flight system, and the conventional SMC controller cannot deal with. Based on the existing problems, the proposed SMCII controller is introduced for the aircraft to achieve better control performance. To guarantee the rationality and persuasion of the comparison, the SMCII is designed based on the SMC controller, and both of them have the same control parameters. Nevertheless, the disturbance observer and the adaptive switch function that introduced to the SMCII controller can significantly improve the control performance. Fig. 11(b) shows the tracking results with the SM-

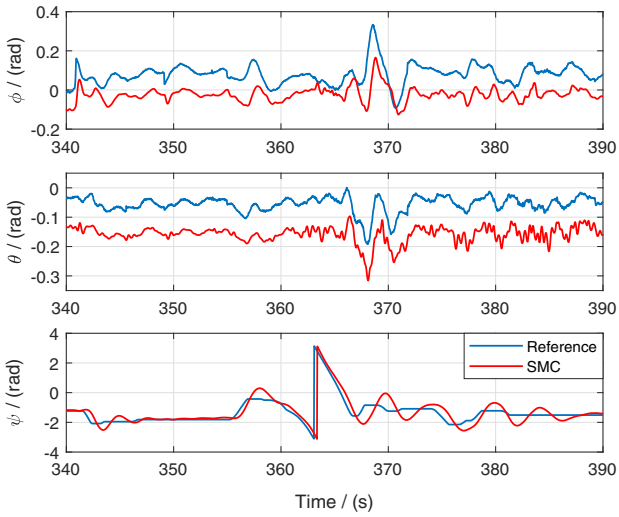

(a) SMC controller.

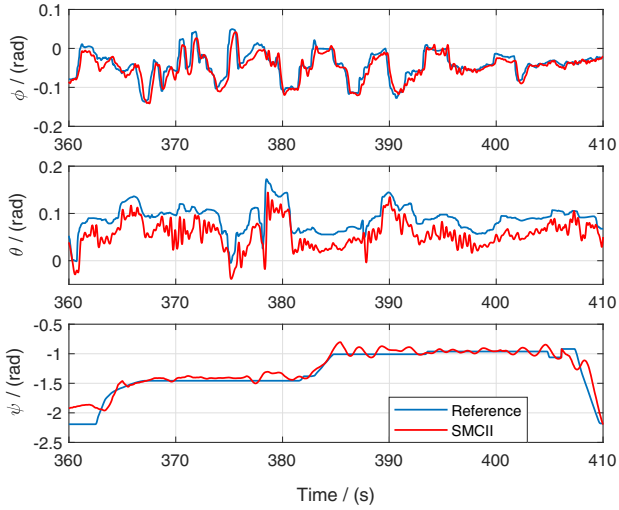

(b) SMCII controller.

Fig. 11. Attitude tracking results.

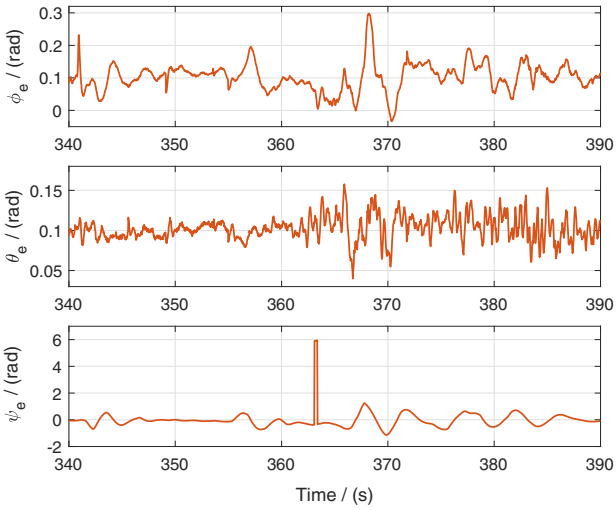

(a) SMC controller.

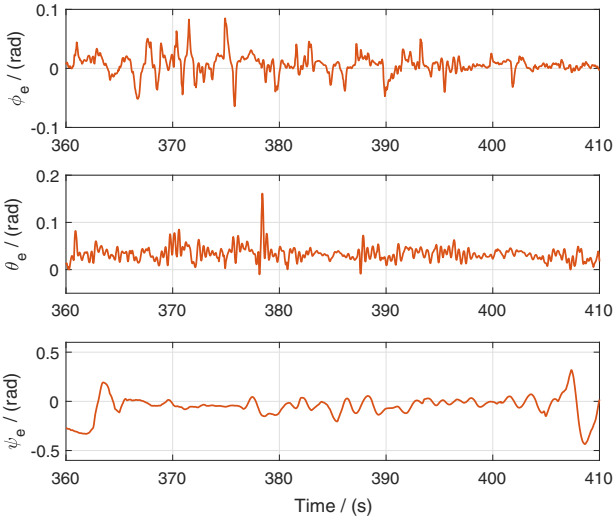

(b) SMCII controller.

Fig. 12. Tracking errors.

CII controller. The tracking errors of the SMCII controller are depicted in Fig. 12(b), and the improvement of the performance can be reflected clearly by comparing with Fig. 12(a). It can be seen that there almost no steady-state tracking error in the roll axis, and the error in the pitch axis is significantly reduced. Besides, the fluctuation of the yaw tracking curve becomes smaller. The IAE indices on three channels are $(5.1375, 5.1323, 16.8067)$ and $(0.6549, 1.6642, 3.9156)$ for the SMC and SMCII, respectively. It is obvious that the performance is improved by the SMCII for all states ($\phi \downarrow 87.25\%, \theta \downarrow 67.57\%, \psi \downarrow 76.70\%$).

The curves of control outputs of different controllers are depicted in Figs. 13 and 14 respectively. From Fig. 13, one can see that the rotation speeds of the two front rotors are different in helicopter mode. Taking the symmetric structure of the aircraft into consideration, it is clear that the installation error and other uncertainties are inevitable in the real flight. The change of the tilting angle is shown in Fig. 14. According to the hierarchical control allocation algorithm, the control of yaw motion is decoupled from the roll and pitch. Namely, the tilting angles are only related to the yaw command Y, and the differential control of the servos is demonstrated clearly. To counteract the moment generated by the rear rotor, the two front rotors always maintaining an angle when hovering. The results illustrate that the proposed control allocation algorithm is useful for the control of the tilt tri-rotor UAV, and the algorithm can be applied for the control of other similar VTOL aircraft. The disturbance estimation results with respect to the three axes are depicted in Fig. 15. The results show that the observer can estimate the disturbance effectively. By using the disturbance estimation for feed-forward compensation, the system performance is improved.

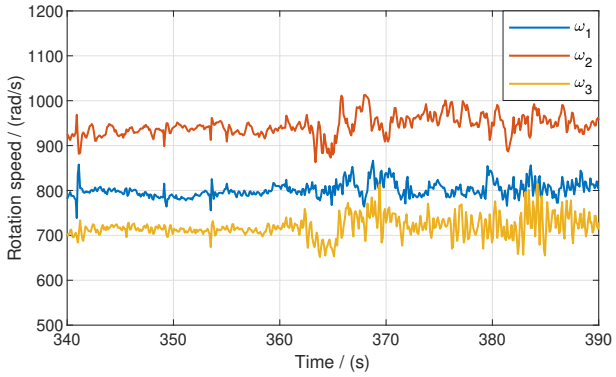

(a) SMC controller.

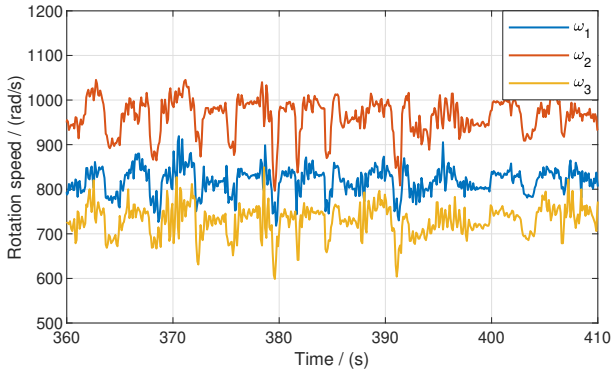

(b) SMCII controller.

Fig. 13. Angular velocity of three rotors.

6. CONCLUSIONS

This paper develops an I&I-based sliding mode controller, which can solve the attitude tracking problem of the tilt tri-rotor UAV subjects to the parameter perturbation, unmodeled dynamics, and external disturbances. To simplify the design of the control system, a hierarchical allocation algorithm is developed to map the input of the individual actuator to the command of the controller. Additionally, the I&I-based observer is constructed to estimate disturbances such that the chattering can be alleviated, and the robustness is enhanced to some extent. Moreover, the dynamic response capability is improved by introducing an adaptive switch function. Finally, simulations are carried out by comparing with other methods to illustrate the performance improvement of the proposed control scheme. Furthermore, the results of the comparative experiments on the platform demonstrate that the SMCII controller can achieve better tracking performance than the SMC controller. Further researches about the mode transition strategy and the uncertainties will be conducted in our future work.

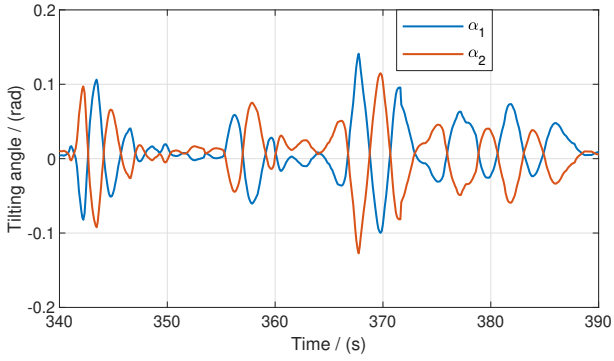

(a) SMC controller.

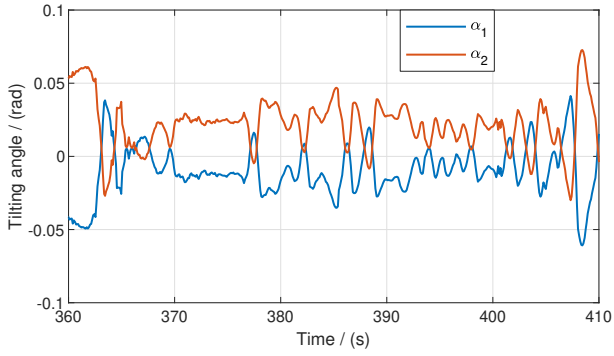

(b) SMCII controller.

Fig. 14. Tilting angle of two front rotors.

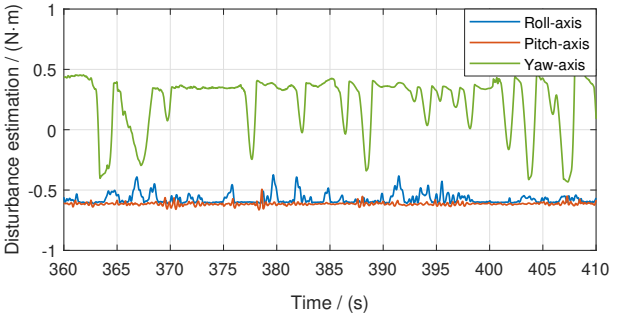

Fig. 15. Disturbance estimation.

REFERENCES

[1] Z. Liu, Y. He, L. Yang, and J. Han, "Control techniques of tilt rotor unmanned aerial vehicle systems: A review," *Chinese Journal of Aeronautics*, vol. 30, no. 11, pp. 135-148, February 2017.

[2] Jr. T. Parham, D. Popelka, D. G. Miller, and A. T. Froebel, "V-22 pilot-in-the-loop aeroelastic stability analysis," *Proc. of American Helicopter Society 47th Annual Forum*, pp. 1307-1319, May 1991.

[3] C. Rago, R. Prasanth, R. K. Mehra, and R. Fortenbaugh, "Failure detection and identification and fault tolerant control using the IMM-KF with applications to the Eagle-Eye

UAV," *Proc. of the 37th IEEE Conference on Decision and Control*, vol. 4, pp. 4208-4213, December 1998.

[4] S. Park, J. Bae, Y. Kim, and S. Kim, "Fault tolerant flight control system for the tilt-rotor UAV," *Journal of the Franklin Institute*, vol. 350, no. 9, pp. 2535-2559, November 2013.

[5] C. S. Yoo, S. D. Ryu, B. J. Park, Y. S. Kang, and S. B. Jung, "Actuator controller based on fuzzy sliding mode control of tilt rotor unmanned aerial vehicle," *International Journal of Control, Automation and Systems*, vol. 12, no. 6, pp. 1257-1265, November 2014.

[6] G. Flores, I. Lugo, and R. Lozano, "6-DOF hovering controller design of the quad tiltrotor aircraft: Simulations and experiments," *Proc. of the 53th IEEE Conference on Decision and Control*, pp. 6123-6128, December 2014.

[7] X. Wang and L. Cai, "Mathematical modeling and control of a tilt-rotor aircraft," *Aerospace Science and Technology*, vol. 47, no. 12, pp. 473-492, December 2015.

[8] N. Liu, Z. Cai, J. Zhao, and Y. Wang, "Predictor-based model reference adaptive roll and yaw control of a quad-tiltrotor UAV," *Chinese Journal of Aeronautics*, vol. 33, no. 1, pp. 282-295, January 2020.

[9] H. Totoki, Y. Ochi, M. Sato, and K. Muraoka, "Design and testing of a low-order flight control system for quad-tilt-wing UAV," *Journal of Guidance Control and Dynamics*, vol. 39, no. 10, pp. 2426-2433, October 2016.

[10] M. Sato and K. Muraoka, "Flight controller design and demonstration of quad-tilt-wing unmanned aerial vehicle," *Journal of Guidance Control and Dynamics*, vol. 38, no. 6, pp. 1-12, October 2014.

[11] L. Zivan, A. Wolff, G. Dekel, and Y. Efraty, "IAI Mini Panther-an Innovative VTOL UAV design," *Proc. of the 54th Israel Annual Conference on Aerospace Sciences*, pp. 1688-1701, February 2014.

[12] Q. Hu, G. Niu, and C. Wang, "Spacecraft attitude fault-tolerant control based on iterative learning observer and control allocation," *Aerospace Science and Technology*, vol. 75, pp. 245-253, February 2018.

[13] Y. Kang, N. Kim, B. S. Kim, and M. J. Tahk, "Autonomous waypoint guidance for tilt-rotor unmanned aerial vehicle that has nacelle-fixed auxiliary wings," *Proc. of the Institution of Mechanical Engineers, Part G: Journal of Aerospace Engineering*, vol. 228, no. 14, pp. 2695-2717, March 2014.

[14] C. Papachristos, K. Alexis, and A. Tzes, "Dual–authority thrust–vectoring of a tri–tiltrotor employing model predictive control," *Journal of Intelligent and Robotic Systems*, vol. 81, no. 3-4, pp. 471-504, March 2016.

[15] K. Alexis, C. Papachristos, R. Siegwart, and A. Tzes, "Robust model predictive flight control of unmanned rotorcrafts," *Journal of Intelligent and Robotic Systems*, vol. 81, no. 3-4, pp. 443-469, March 2016.

[16] A. Prach and E. Kayacan, "An MPC-based position controller for a tilt-rotor tricopter VTOL UAV," *Optimal Control Applications and Methods*, vol. 39, no. 1, pp. 343-356, January 2018.

[17] H. Ríos, R. Falcón, O. A. González, and A. Dzul, "Continuous sliding-mode control strategies for quadrotor robust tracking: Real-time application," *IEEE Transactions on Industrial Electronics*, vol. 66, no. 2, pp. 1264-1272, April 2018.

[18] Y. Zou, "Nonlinear robust adaptive hierarchical sliding mode control approach for quadrotors," *International Journal of Robust and Nonlinear Control*, vol. 27, no. 6, pp. 925-941, March 2017.

[19] J. Pan, W. Li, and H. Zhang, "Control algorithms of magnetic suspension systems based on the improved double exponential reaching law of sliding mode control," *International Journal of Control, Automation and Systems*, vol. 16, no. 6, pp. 2878-2887, December 2018.

[20] H. Du, J. Zhang, D. Wu, W. Zhu, H. Li, and Z. Chu, "Fixed-time attitude stabilization for a rigid spacecraft," *ISA Transactions*, vol. 98, pp. 263-270, March 2020.

[21] S. Ding, K. Mei, and S. Li, "A new second-order sliding mode and its application to nonlinear constrained systems," *IEEE Transactions on Automatic Control*, vol. 64, no. 6, pp. 2545-2552, August 2018.

[22] A. Astolfi, and R. Ortega, "Immersion and invariance: A new tool for stabilization and adaptive control of nonlinear systems," *IEEE Transactions on Automatic Control*, vol. 48, no. 4, pp. 590-606, April 2003.

[23] Y. Zou and Z. Meng, "Immersion and invariance-based adaptive controller for quadrotor systems," *IEEE Transactions on Systems, Man, and Cybernetics: Systems*, vol. 49, no. 11, pp. 2288-2297, January 2018.

[24] J. Y. Lau, W. Liang, and K. K. Tan, "Adaptive sliding mode enhanced disturbance observer-based control of surgical device," *ISA Transactions*, vol. 90, pp. 178-188, July 2019.

[25] Y. Yang and Y. Yan, "Neural network approximation-based nonsingular terminal sliding mode control for trajectory tracking of robotic airships," *Aerospace Science and Technology*, vol. 54, pp. 192-197, July 2016.

[26] D. F. Zhang, S. P. Zhang, Z. Q. Wang, and B. C. Lu, "Dynamic control allocation algorithm for a class of distributed control systems," *International Journal of Control, Automation and Systems*, vol. 18, no. 2, pp. 259-270, February 2020.

[27] T. A. Johansen, and T. I. Fossen, "Control allocation—a survey," *Automatica*, vol. 49, no. 5, pp. 1087-1103, May 2013.

[28] Y. Seo and Y. Kim, "Modeling and attitude control of tri-tilt ducted fan vehicle," *Proc. of the AIAA Guidance, Navigation, and Control Conference*, January 2016.

[29] G. Di Francesco, M. Mattei, and E. D'Amato, "Incremental nonlinear dynamic inversion and control allocation for a tilt rotor UAV," *Proc. of the AIAA Guidance, Navigation, and Control Conference*, January 2014.

[30] J. Zhang, P. Bhardwaj, S. A. Raab, S. Saboo, and F. Holzapfel, "Control allocation framework for a tilt-rotor vertical take-off and landing transition aircraft configuration," *Proc. of the 2018 Applied Aerodynamics Conference*, June 2018.

[31] J. Hu, and H. Zhang, "Immersion and invariance based command-filtered adaptive backstepping control of VTOL vehicles," *Automatica*, vol. 49, no. 7, pp. 2160-2167, July 2013.

[32] L. Yu, D. Zhang, J. Zhang, and C. Pan, "Modeling and attitude control of a tilt tri-rotor UAV," *Proc. of the 36th Chinese Control Conference*, pp. 1103-1108, July 2017.

Li Yu received his B.S. degree from Shandong University, China, in 2015 and M.S. degree from the National University of Defense Technology, China, in 2017, where he is currently pursuing his Ph.D. degree. His research interests include robust control, adaptive control, and unmanned aerial vehicles.

Guang He received his B.S. degree from Northeastern University, China, in 2008, and his M.S. and Ph.D. degrees from National University of Defense Technology, China, in 2010 and 2016, respectively. He is currently a lecturer at the National University of Defense Technology. His research interests include unmanned aerial vehicles and nonlinear control.

Shulong Zhao received his B.S. degree from Beihang University, China, in 2011, and his M.S. and Ph.D. degrees from National University of Defense Technology, China, in 2013 and 2017, respectively. He is currently a lecturer at the National University of Defense Technology. His research interests include data-driven control and curved path following of UAV.

Xiangke Wang received his B.S., M.S., and Ph.D. degrees from National University of Defense Technology, China, in 2004, 2006, and 2012, respectively. From 2012, he is with the College of Intelligence Science and Technology, National University of Defense Technology, China, as a full professor. His research interests include multi-agent systems, nonlinear control, and unmanned aerial vehicles.

Lincheng Shen received his B.S., M.S., and Ph.D. degrees in automatic control from the National University of Defense Technology, China, in 1986, 1989, and 1994, respectively. In 1989, he joined the Department of Automatic Control, NUDT, where he is currently a full professor. He has been serving as an Editorial Board Member of the Journal of Bionic Engineering since 2007. His research interests include unmanned aerial vehicles, swarm robotics, and artificial intelligence.